Computer simulations of damage due to passage of a heavy fast ion through diamond

A. Sorkin,* Joan Adler, and R. Kalish

Physics Department, Technion, Israel Institute of Technology, 32000 Haifa, Israel

(Received 17 July 2003; revised manuscript received 12 January 2004; published 31 August 2004)

We present tight-binding molecular dynamics simulations of the structural modifications that result from the "thermal spike" that occurs during the passage of a heavy fast ion through a thin diamond or amorphous carbon layer, and the subsequent regrowth upon cooling. The thermal spike and cooling down are simulated by locally heating and then quenching a small region of carbon, surrounded either by diamond or by a mostly sp^3 bonded amorphous carbon network. For the case of the thermal spike in diamond we find that if the "temperature" (kinetic energy of the atoms) at the center of the thermal spike is high enough, an amorphous carbon region containing a large fraction of threefold coordinated C atoms (sp^2 bonded) remains within the diamond network after cooling. The structure of this amorphous layer depends very strongly on the "temperature" of heating and on the dimensions of the thermal spike. Scaling is found between curves of the dependence of the percentage of sp^2 bonded atoms in the region of the thermal spike on the heating "temperature" for different volumes. When the thermal spike occurs in an initially amorphous sample the structure of the damaged region after cooling exhibits the above dependencies and is found to be a function of the structure of the original amorphous carbon layers.

I. INTRODUCTION

Carbon can bond in different hybridization forms, including diamondlike (sp^3) and graphitelike (sp^2), resulting in C based materials with extremely different physical and chemical properties. After equilibrium conditions are achieved, disrupted sp^3 bonds may reconstruct as the more stable sp^2 bonds. The passage of swift ions through matter causes heating to very high temperatures which results in severe bond breakage. This local damage around the ion track is generally referred to as a "thermal spike" which accompanies the stopping of the ion in matter. For the case of diamond, the local bond disruption of the sp^3 bonds, and subsequent reconstruction upon equilibrium, may result in the formation of an sp^2 rich region along the ion track. Indeed, the passage of MeV or GeV heavy ions through diamondlike (sp^3 rich) layers has been shown by high resolution AFM and STM scans to result in local graphitization.[1] This is supported by the formation of protrusions at the ion-impact points (swelling) and by the formation of electrically conductive channels along the ion track. Both these modifications of the diamond indicate that preferred sp^2 bonding has occurred along the pathways of the ions, in the otherwise sp^3 rich material.[2] The width of the transformed material, due to the impact of GeV Au ions, has been deduced from the data and was found to be of the order of 85 nm. Figure 1 illustrates the material transformation (density and electrical conductivity) measured by atomic force and scanning tunneling microscopy.

The damage inflicted on diamond by the passage of sub-MeV ion is known to result in electrically conductive regions along the ion track and around the stopping points of the ions.[3] At high enough implantation doses the individual damage tracks overlap resulting in the formation of macroscopic conductive regions, which have been shown to give rise to hopping conductivity. The exact structure of these damaged regions in diamond is controversial. Prins postulates that

they mainly contain a mixture of vacancies and interstitial C atoms which eventually collapse to form vacancy clusters (vacloids).[4] On the other hand, Prawer and Kalish have concluded, based on measurements of the dependence of the conductivity of damaged diamond on ion-damage-implantation dose, that the ion-affected diamond at high enough doses is highly conductive due to the formation of graphitelike regions along the ion tracks.[5]

Computer simulations of the damage in diamond caused by the energetic displacement of a few C atoms resulting in damage to a small volume in diamond[6] (of 1.4 nm^3) show that the size and nature of these regions depend on the initial recoil energy imparted to the C atoms and on the sample temperature. In some cases, when the sample was heated to 3000 K the formation of clusters of sp^2 bonded C atoms forming sixfold rings has been observed in these simulations.

In the present study we simulate the passage of a swift ion through a diamond or a diamondlike tetrahedrally bonded amorphous C (named *ta-C*) layer by locally "heating" a section of the sample up to very high temperatures (comparable to the temperatures expected to prevail in the thermal spike). The temperatures studied are between 14 000 and 30 000 K, corresponding to kinetic energies of 1.2 to 2.6 eV per atom
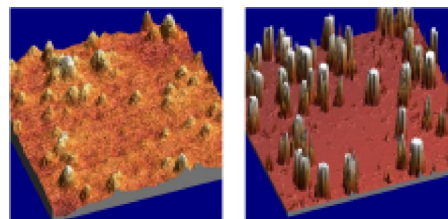

FIG. 1. (Color online) Surface morphology (left-hand side) and local electrical conductivity (right-hand side) of the transformed diamondlike amorphous carbon due to ion impact (taken from Ref. 2).

which are of the order of the energies delivered to the recoiling carbon atoms within the damage cascade, as obtained[7] by SRIM simulations (see next section). These energies, obviously, depend on the details (energy and mass) of the ions that cause the "thermal spike."

We compute the sp^2 and sp^3 fractions in the affected volume and follow their evolution as a function of cooling rate and time. For the samples that were initially diamond structure we find that, upon cooling, a region which contains both sp^2 and sp^3 bonded C forms along the track. The nature of the material in this regrown region depends on the initial heating of the track and on its cooling rate. Under some conditions, complete regrowth back to perfect diamond is found, whereas in other cases, a sp^2 rich region remains along the ion track. Similar results are found when a thermal spike is simulated in initially amorphous carbon which is then allowed to cool down under a range of different conditions. The relevance of these computational results, despite the obvious limitations of small samples, defect "track" configuration and relatively short cooling times, is their resemblance to the conditions expected to prevail within the thermal spike and its rapid quenching during cooling. Slow bond rearrangements at low ($\sim$1000 C) temperatures, as obtained by thermal annealing, are not considered here.

We start below by briefly reviewing the physical processes involved in the formation of the thermal spike and the typical parameters of such a spike initiated in diamond by the passage of a swift heavy ion; we then describe the computations performed, discuss their relevance to ion-implantation experiments and present and discuss our results.

II. BACKGROUND

The "thermal spike" which accompanies the passage of an ion through matter can be viewed as a short-time local melting of the ion damaged region followed by a rapid cooling. Quenching from the liquid phase has been widely used to create amorphous materials (including amorphous carbon) in computer simulations, using empirical potentials,[8] and *ab initio*[9–11] and tight-binding molecular dynamics.[12–14] It has been shown that such a procedure produces an amorphous carbon similar to material produced experimentally by the deposition of a carbon film either by evaporation in an electron beam, by carbon arc[15–17] or by ion beam deposition with ion energies between several ten and several hundred eV.[18–20].

In contrast to this large body of computer simulations of amorphous carbon, there have been only a few simulations of the material resulting from damaging diamond by ion implantation. Specific simulations of damage in material induced by ion implantation can be divided into two categories: (i) the commonly used TRIM code[21,22] or its more recent version SRIM[7] and (ii) the molecular dynamics (MD) technique.[23]

The TRIM (TRansport of Ions in Matter) code is a Monte Carlo program that calculates the trajectories of the primary ion and of the recoiling host atoms involved in the irradiation event. The required input parameters are the ion type and energy and the properties of the host material, i.e., its com-

position, density, and the displacement energy of the constituent atoms. TRIM provides good estimates of the damage and of the implant distributions and it is widely used in planning the dopant profile in ion-implantation experiments. However, TRIM cannot account for the structure of the material (amorphous vs crystalline) nor model the dynamic annealing of the implantation affected material. In particular, it cannot predict the nature of the defects in diamond because of the variety of possible bonding configurations of carbon that may induce the diamond to graphite transition. It is worth mentioning that recently significant efforts were directed toward the extension of the capabilities of TRIM. For example, the Crystal-TRIM program[24] can take into account crystallinity of the target. A modification of TRIM has recently been developed by Sha'anan[22] which enables following the evolution, in space and time, of the damage cascade caused by the passage of a single ion through matter. The results of the application of this code to simulate the passage of an 1 MeV Xe ion through diamond show that extremely high temperatures (of the order of many tens of thousand of degrees) are induced during very short times (less than 1 ps) along the ion track. As we will discuss below, these resemble the time/temperature regime modeled in our computations of the damage inflicted on diamond and *ta-C* (tetrahedral amorphous carbon) by heavy ion irradiation.

Recently, an improved version of TRIM that simulates the energy loss of swift ions, SRIM (The Stopping and Range of Ions in Matter) code[7] was developed. This code calculates the stopping and range of ions slowing down in matter using a quantum mechanical treatment of ion-atom collisions. This calculation is made very efficient by the use of statistical algorithms which allow the ion to make jumps between calculated collisions and then averaging the collision results over the intervening gap. For example, the stopping power of fast He, Be, C, and Al ions in carbon in a wide range of energy was calculated and the values were found to agree with experimental results within a few percent.[25]

A MD study of radiation damage caused by the passage of a single carbon atom through diamond was performed by Wu and Fahy,[26] using the Tersoff potential. In that study the computations were restricted to the investigation of the damage threshold energy necessary to displace a single C atom from its lattice site. Smith[27] simulated the results of the bombardment of diamond using a similar computational method but limiting the analysis to the ejection mechanisms of C atoms from a diamond surface (carbon self-sputtering). Marks[28] has investigated the growth of *a-C* layers. By computing the mean square displacement of the atoms during the cooling of the melt and the time required for it to relax, the life-time of the thermal spike in diamond was found to be less than 1 picosecond, for ion impacts below 400 eV. In this latter study *ab initio* MD techniques were used.

Saada *et al.*[6] carried out MD simulations, using the Tersoff potential, of a damage region embedded inside a diamond matrix created by the energetic displacement of carbon atoms with a kinetic energy of up to 416 eV (8 times the displacement energy of carbon atoms in diamond) in the bulk of a diamond crystal. Such regions are likely to appear in diamond at the final stages of the implantation-related damage cascade. In these simulations the temperatures of the

"thermal spike" are extremely high, and last for very short times, hence the effects of the temperature at which the samples are held (the so-called implantation temperature) is negligible within these simulations. We note that further annealing of the damaged region will occur, but over a much longer time scale. [Depending on the sample macroscopic temperature and on the diffusivities of the annealing species (whether vacancies or interstitials) the relaxation times of the crystal into its final "room temperature" state may last as long as fractions of seconds. This time regime and the annealing taking place in it are not dealt with here.] The conclusion of the Saada *et al.* study was that partial amorphization of a volume with a radius of $1-2$ nm occurs around the stopping point of the recoiling ion. With an increasing number of successively displaced atoms, the damage volume and the number of threefold coordinated atoms was found to increase. The structure of the damaged regions (i.e., the ratio of sp^2 and sp^3 bonded C atoms) was found in Ref. 6 to depend on the sample temperature.

These computer studies strengthen our understanding of the processes occurring inside or at the end of an ion track in diamond. However, the transitions from sp^3 to sp^2 bonds within thermal spike regions have not yet been investigated in detail. The purpose of the present study is to investigate transformations of diamond and diamondlike amorphous carbon under the extreme conditions which prevail during and after the passage of a heavy fast ion through the material.

III. TIGHT-BINDING SIMULATION DETAILS

A. General description of the calculations

We present simulations of the thermal spike which occurs during the passage of a heavy fast ion through either diamond or amorphous carbon by locally heating a slab of the material to very high temperatures and allowing it to rapidly cool down. It should be mentioned, that because of computational limitations, we have simulated the damaged region as a slab of molten material sandwiched between cold undamaged layers rather than more realistic cylindrical shape of an ion track. Nevertheless the general trends found here should also hold for the cylindrical geometry. A large increase in volume accompanies the sp^3- to sp^2-bond conversion,[29] but the volume of the damaged region in the center of the diamond is restricted by the surrounding diamond (or amorphous carbon) lattice, therefore simulations are carried out under constant volume conditions. In order to set the initial temperature, a randomly directed velocity is assigned to each atom. The value of the velocity is randomly selected in accordance with a Maxwell distribution for the desired temperature. The velocities can be rescaled to be related to the ambient temperatures. Periodic boundary conditions are applied to the samples in all three directions. The MD step was 0.5×10^{-15} s. In order to describe the interactions between carbon atoms we use a tight-binding model,[30] which has been shown to be transferable to successfully simulate different carbon polytypes: diamond, graphite, fullerenes[31] as well as disordered carbon structures such as liquid and amorphous carbon phases.[12,13].

The method used here to distinguish between sp^3 and sp^2 bonded atoms is based on determination of the coordination number of each atom. The radial distribution function (RDF) of all carbon samples exhibits a clear gap, centered at about 0.19 nm, separating the first and the second peak corresponding to the first and second neighbor shells. All atoms within the sphere of radius 0.19 nm are thus assumed to comprise the nearest neighborhood of a given atom. Therefore, the number of neighbors of each atom within a distance of 0.9 nm determines the coordination number. Atoms that have four nearest neighbors within this sphere are assumed to be sp^3 bonded, atoms which have three nearest neighbors are assumed to be sp^2 bonded and atoms which have only two are assumed to be sp bonded. No atoms with higher coordination number were found during the simulations.

The Atomic Visualization package (**AViz**)[32] was used extensively in all stages of this project. Visualization of our carbon samples with color coding for different atomic bonding helped identify clusters of either sp^2 or sp^3 coordinated atoms, rings, graphitelike planes. Color pictures of the results of the present study can be found in the online version and animations are also presented on the web site.[33]

B. Details of the sample preparation

1. Damaged diamond sandwiched between two layers of diamond

Six different samples with a density of 3.5 g/cc, initially arranged as a perfect diamond crystal, were prepared. Their sizes were $2 \times 2 \times 6$ (192 atoms), $2 \times 2 \times 7$ (224 atoms), 2×8 (256 atoms), $2 \times 3 \times 6$ (288 atoms) and $3 \times 3 \times 6$ (432 atoms) diamond unit cells.

The "thermal spike" was created by heating the central layers up to "temperatures" of $1.2-2.6$ eV $(14\,000-30\,000$ K). The 32 upper and 32 lower atoms of each sample (the upper and lower layers of a height of 3.55 Å) were frozen, i.e., the motion of these atoms was forbidden. The initial geometry of the samples is shown in Fig. 2. The outermost frozen diamond layers had the effect on their neighboring hot atoms of forcing them to return to their initial positions, i.e., to regrow epitaxially back to diamond. In this way a temperature gradient from the edges to the center of the sample was created. Once the liquid phase reached equilibrium (this process was controlled by monitoring the total energy of the system), the central layers were cooled to room temperature at a cooling rate of 10 K/fs. This cooling rate was selected after a number of earlier simulations carried out at slower cooling rates showed that the final sp^2/sp^3 ratio is not sensitive to this specific characteristic of the cooling process. The height of the hot layers varied between four and six diamond unit cells (not at the expense of the height of the outer cold layers) and the width of the hot layers varied from two to three diamond unit cells. The full time of cooling was 1.5 ps (3000 MD steps). However, the central layers ceased to move after the 750 first MD steps, so the lifetime of our "thermal spike" was 0.3 ps. This value is similar to the lifetime estimates of Marks[28] and Saada,[6] of 0.2 ps and 0.21 ps, respectively.
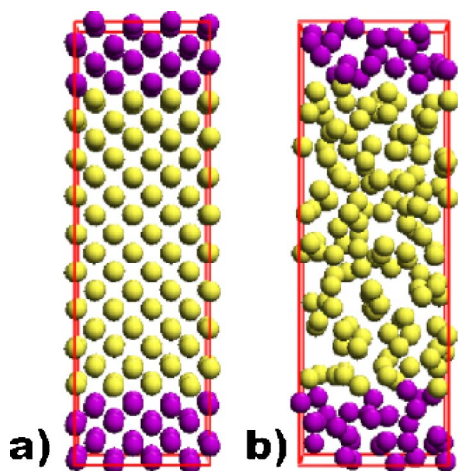
FIG. 2. (Color online) Initial configurations of the samples: (a) crystalline diamond sample, (b) ta—C sample; grey (purple online) balls represent the frozen atoms, white (yellow online) balls represent atoms that are free to move.

2. Damaged amorphous C region sandwiched between two layers of frozen ta—C

Four initial samples of diamondlike amorphous carbon at density 3.5 g/cc were prepared by heating diamond up to 5000 K followed by cooling of the liquid phase to 300 K during 5 ps with an exponential cooling profile. Each ta—C amorphous sample contained 192 atoms with a geometry 7.1 Å×7.1 Å×21.3 Å. The samples contained 66±4 % of sp^3 coordinated atoms. In order to achieve a larger percentage of sp^3 coordinated atoms (above 70%), two additional samples were prepared using the the following procedure: the amorphous structure was prepared with a density of 4.0 g/cc by quenching a liquid phase down from 10 000 K 700 K with a cooling rate of about 500 K/ps, then the density was reduced from 4 to 3.5 g/cc by uniform expansion, after which the temperature of the system was raised to 2500 K, and thereafter the structure was recooled to room temperature.[13] The two structures obtained at a final density of 3.5 g/cc consisted of 84% and 77.5% of sp^3 bonded atoms, respectively.

To simulate a "thermal spike" in the diamondlike amorphous carbon samples, the central region of each sample was heated to "temperatures" of 1.2–2.60 eV per atom (14 000–30 000 K). The upper and lower layers of a height of 3.55 Å each, were kept frozen. For the six amorphous carbon samples the height of the hot layers was 14.2 Å (128 atoms in average). A representation of a typical initial sample geometry is given in Fig. 2. Dark (purple online) atoms at top and bottom indicate the frozen layers, the light (yellow online) central ones are free to move and during heating, there is a temperature gradient from the edges to the center of the samples. Following the heating stage the structures were cooled to room temperature at a cooling rate of 10 K/fs. The time of calculations and the lifetime of the "thermal spike" were the same those described above for the case of the damaged region between two layers of perfect diamond.

C. Sample equilibration

We checked carefully, by monitoring of the total energy of the system, that the heating time was sufficiently long to enable the liquid structure to reach equilibrium (early attempts to prepare samples of amorphous carbon by quenching from a liquid carbon that was not in equilibrium led to inconclusive results).

D. Relevance to experiment

Our aim is to determine the nature of transitions between different carbon bonds as the result of the passage of fast ions in samples of different initial structures. To do this, we need to examine the region of passage and its intermediate neighborhood on an atomistic scale. However, this microscopic region is contained in a larger carbon matrix, and while the microscopic region corresponds directly to that in the experiment, the surrounding matrix may differ in scale. We address the issues of system size and temperature in relation to the parameters of experimental samples.

In the simulations, on one hand, a maximum of 432 atoms can be contained in a single sample due to computational limitations. On the other hand, the periodic boundary conditions mean that the sample is in a sense infinite, and, in particular, has no surfaces. Thus the simulation samples are both smaller and larger than the laboratory experiment. We note that a slab of modified material sandwiched between frozen layers is simulated instead of a cylinder, which would better resemble the shape of the disrupted region around an ion track. This simplification does not influence the qualitative results, since we are investigating the local region around the ion path (which has a linear extent of 7.2 Å along the track direction and repeated periodically in this direction). The geometry was chosen so that this region is well surrounded, in the direction perpendicular to the track, by diamond or amorphous carbon matrix, which is frozen in place. In particular, there are 7.4 Å between replicas of the tracks, a region that is sufficient to avoid interaction since the range of the potential is only 3 Å. In order to ensure that the samples are of sufficient size to enable reliable interpretations, a series of different sizes were used for each situation and the effect of the scaling of the system size was carefully investigated. This is not exactly equivalent to the finite size scaling[34] that is commonly applied to phase transitions and critical phenomena, and is closer to the scaling used by Rosenblum et al.[35] in a study of thermal stress at diamond interfaces. The excellent agreement of both of these scaling approaches with results from laboratory experiments gives us confidence in the concept. The data collapse, as a function of system size, and the smoothness of the scaling that will be demonstrated below confirms that the results could be reliably extrapolated even further if needed.

Temperature is introduced into the simulations as kinetic energy. In the laboratory, the region around the ion track is extremely hot for a very short time. The high heating "temperatures" of the simulation are thus large amounts of kinetic energy given to the heated atoms. Again here, we have studied the scaling of "temperature" with system size. Not surprisingly, the actual "temperature" needed to attain specific

TABLE I. Fraction of the fourfold, threefold, and twofold coordinated atoms in the heated layer after cooling in the sample with 192 atoms.

T (eV/atom)	Fourfold (%)	Threefold (%)	Twofold (%)
1.55 eV	100	0	0
1.72 eV	95±5	5±5	0
1.98 eV	79±5	19±5	2±2
2.41 eV	74±5	23±5	3±2
2.58 eV	62±5	34±5	4±3

structures is a function of system size. Again, collapse of graphs to a single functional form will be demonstrated and provides validation for our approach.

IV. RESULTS OF TIGHT-BINDING SIMULATIONS

A. Damaged diamond sandwiched between two layers of intact diamond

1. Influence of the heating "temperature"

When the diamond lattice in the central hot layers was melted, C-C separations, that resemble those between sp^2 and sp bonded atoms, appeared in the liquid layers. Upon cooling some (or all) of these sp^2 and sp bonded atoms transformed back to sp^3 coordinated C atoms. The final fraction of threefold and twofold coordinated atoms depends on the kinetic energy per atom ("temperature") in the heating process. The higher the heating "temperature" of the atoms the larger was the ratio of sp^2/sp^3, that prevailed after cooling. Samples initially heated to a relatively low "temperature" returned to diamond, whereas for hotter samples some non-diamond bonds remained after cooling.

For example, let us consider the $2 \times 2 \times 6$ sample containing 192 atoms, 128 of which were free to move (i.e., were heated and subsequently cooled). The percentages of fourfold, threefold, and twofold coordinated atoms in the hot layers after cooling from different "temperatures" are presented in Table I. Whenever the heating "temperature" was

FIG. 4. The fraction of threefold coordinated atoms in the hot layers, shown during the process of cooling from the initial "temperature" of 1.725 eV and 1.98 eV/atom. The sample contained four hot layers (128 atoms). Each MD step is 0.5×10^{-15} s.

lower than 1.72 eV per atom all sp^2 and sp bonds disappeared in the process of cooling, and the final, cooled, structure returned to a perfect diamond lattice, as shown in Fig. 3 where the percentages of different hybridizations are graphed as a function of "temperature" during the cooling process.

At higher initial heating "temperatures" the heated layers remained, after cooling, partially or entirely amorphous. The fraction of threefold and twofold coordinated atoms in the structure does not disappear. Figure 4 shows the percentages of sp^2 bonded atoms during the cooling process from different initial heating "temperatures:" at low initial temperature whole sample returns to diamond and a percentage of sp^2 bonded atoms decreases to zero, at high initial temperatures amorphous phase with presence of sp^2 (and sometimes sp) coordinated atoms remains in the center of the sample. It should be mentioned that the specific bonding configurations become meaningful only once the sample starts to solidify.

The volume of the region remaining amorphous after cooling was found to increase with the heating "temperature." In Fig. 5 visualizations of some samples cooled from
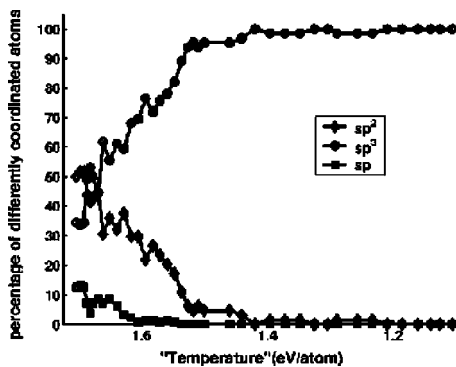

FIG. 3. Recovery rate showing the evolution of the fraction of twofold, threefold, and fourfold coordinated atoms in four layers (128 atoms) during the cooling process, following heating to 1.725 eV.
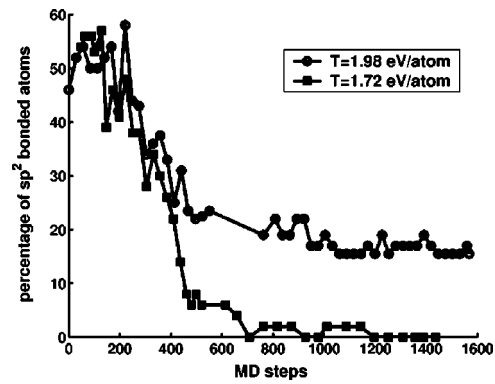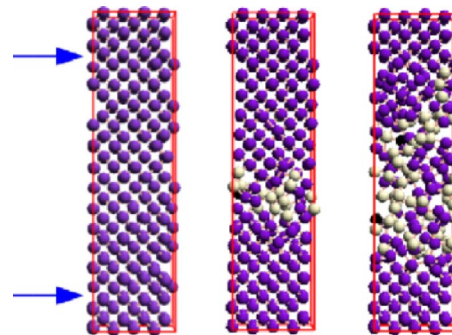

FIG. 5. (Color online) Amorphous carbon located between two layers of diamond. The samples contained 192 atoms ($2 \times 2 \times 6$), temperature of heating was 1.2 eV/atom (left), 1.38 eV/atom, (center) and 1.98 eV/atom (right). Grey (purple) balls represent fourfold coordinated atoms, white (yellow) balls represent threefold coordinated atoms, black balls (which appear only in the right most sample) represent twofold coordinated atoms. Boundaries between frozen layers and layers of atoms which are free to move are denoted by arrows. (Purple and yellow are shown online.)
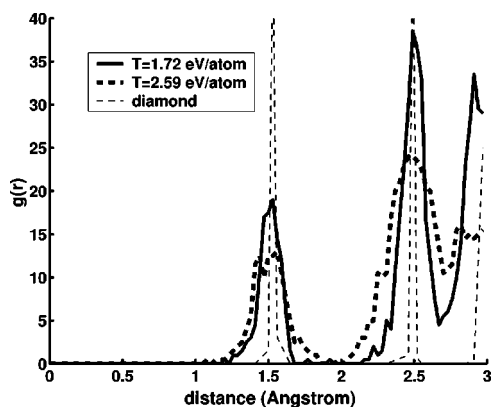
FIG. 6. Radial distribution functions $g(r)$ of the central layers of the sample containing four hot layers ($2 \times 2 \times 6$) cooled from two different initial "temperatures." The thin dashed line shows the radial distribution function of the initial diamond sample for comparison.
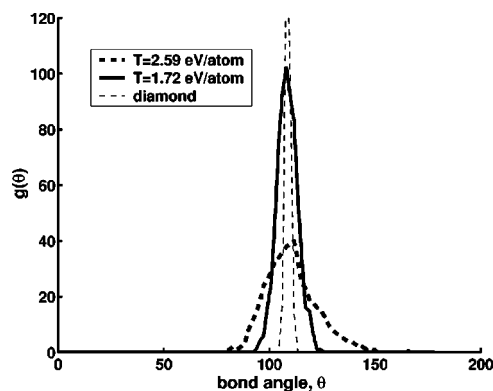

FIG. 7. Angular distribution functions of the central layers of the sample containing four hot layers ($2 \times 2 \times 6$), cooled from two different initial "temperatures." The thin dashed line shows the angular distribution function of the initial diamond sample for comparison.

different heating "temperatures" are presented. We see that in the sample where the heating "temperature" was high (1.98 eV/atom) almost an entire layer of atoms which were free to move has transformed to amorphous carbon with 19% of sp^2 bonds, while in the sample initially heated to 1.38 eV/atom only a small central region is amorphous and the layers which are adjacent to the frozen part of the sample return to their crystalline diamond structure. The reason for the dependence of the volume that remains amorphous on heating "temperature" is that at lower "temperatures" the frozen outer layers of diamond extend their influence to larger distances, therefore a larger volume of the damaged region reconstructs to the diamond structure after cooling. A tendency to segregation of the threefold and the fourfold atoms was observed in the samples heated to high temperatures when the volume of the region that remained amorphous was sufficiently large (almost all nonfrozen atoms).

The radial distribution function (RDF) of the C atoms in the hot layers is presented in Fig. 6. For high heating "temperatures" the overlapping subpeaks that make up the first peak located at ~1.5 Å are a superposition of two peaks that correspond to the first nearest neighbors of sp^2 bonded (located at ~1.42 Å) and sp^3 bonded atoms (located at ~1.54 Å). The second peak located at 2.5 Å, representing second nearest neighbors, is high due to the layers which have reconstructed to diamond structure after cooling. However, as was explained above, the higher the "heating temperature" the larger the volume of the region remaining amorphous. Therefore all RDF peaks related to the higher

TABLE II. Fraction of the fourfold, threefold, and twofold coordinated atoms in the samples with different height of the hot layer heated to 1.72 eV per atom.

Number of layers	Fourfold (%)	Threefold (%)	Twofold (%)
4	95±5	5±5	0
5	78±5	21±5	1
6	74±5	26±5	0–2

heating "temperature" (dashed line) are lower and broader.

The angular distribution function of the hot layers demonstrates similar behavior, see Fig. 7. The peaks are lower and broader when the heating "temperature" is higher, this corresponds to a higher fraction of threefold and twofold coordinated atoms. The angular distribution peak related to $T=1.98$ eV is located at 112° (closer to the ideal 120° for sp^2 bonded C atoms), while the peak of the curve related to 1.72 eV is located at 109° (typical for sp^3 bonded atoms).

2. Effects of the size of the hot layers

The heating "temperature" is not the only factor that influenced the structure of the damaged region. If the height of the layer with atoms that were free to move was increased from four to six unit cells without changing the width of samples, the percentage of threefold and twofold coordinated atoms in the damaged layers, when heated to the same temperature also increased (see Table II). As was explained above, the frozen layers assist the intermediate layers in their vicinity to return to diamond lattice structure. The central atoms in the samples with a large number of the hot layers feel the influence of the diamond frozen layers to a lower extent, and therefore the volume of the region remaining amorphous after cooling was large, with a high percentage of sp^2 coordinated atoms. In the small samples the central layers needed to be heated to very high "temperatures" to diminish the influence of the outer frozen layers. The highest "temperature" at which the sample reconstructed its diamond lattice after cooling also depended on the height of the hot layers. This temperature decreased as the height of the hot layers increased (see Table III).

Graphs of the dependence of the percentage of sp^2 bonded atoms on the heating "temperature" are plotted in Fig. 8 for the samples with different heights and same width of the hot layers. Interestingly, all these curves have the same shape for different numbers of the hot layers despite the different distances between the hot layers and the frozen ones. All the curves can be fitted to a unique function $f(T-T^*)$, where T^* is the upper temperature of heating, at which the sample can

TABLE III. The upper "temperature" of heating at which the samples reconstruct their diamond structure ($T*$).

Number of layers	$T*$
4	1.63 ± 0.04 eV
5	1.51 ± 0.04 eV
6	1.38 ± 0.04 eV

return to diamond after cooling. In Fig. 9 the collapse of the curves to a single scaling function is shown.

The samples with different width (from 32 to 72 atoms in each layer) at the same height of the hot layers also demonstrate finite size effects. The percentage of threefold and twofold coordinated atoms in the central layers is larger in the wider samples at the same heating "temperature," the "temperature" at which the sample returns to diamond, $T*$, is higher for the thinner samples (see Table IV).

B. Simulation of molten and cooled amorphous carbon located between two frozen layers of amorphous carbon

Now let us consider structure of a central amorphous carbon layer sandwiched between two layers of frozen amorphous carbon. After cooling, the central damaged region remained amorphous, but the sp^2/sp^3 ratio changed. The dependence of this generated structure on the heating "temperature" was similar to that of the previous stage of the simulation (amorphous carbon between two layers of diamond). Namely, if the central atoms were heated to higher "temperatures," the fraction of the sp^2 bonded atoms increased (correspondingly, the fraction of the sp^3 bonded atoms decreased). Some of these structures were highly inhomogeneous, in particular when the initial sample contained a large fraction of fourfold bonded atoms and was heated to a relatively high "temperature." In Fig. 10 the visualization of some of these amorphous carbon samples is presented. We can see that the frozen layers of the sample with 77.5% of sp^3 bonded atoms initially, contained after heating and subsequent cooling 75% of sp^3 bonded atoms, while the central layers after heating to 2.33 eV and subsequent quenching contained only 39% of the fourfold atoms.
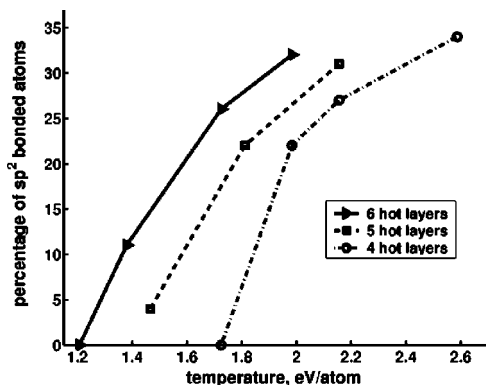

FIG. 8. The dependence of the percentage of sp^2 bonded atoms on the heating temperature for different heights of the hot layers.
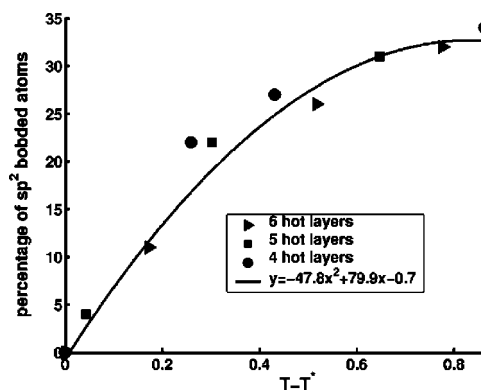

FIG. 9. The same curves shifted to $T*$. The solid line is a result of square polynomial fitting.

The radial (RDF) and the angle (ADF) distribution functions of the central layers of this amorphous carbon sample after cooling from the "temperatures" of 1.55 eV and 2.33 eV are plotted in Figs. 11 and 12, respectively. The peaks corresponding to the higher temperatures of heating were lower, broader, and slightly shifted toward the shorter, graphite, bond length and larger, graphitelike, bond angle relative to those at the lower temperatures. This indicates a higher fraction of the sp^2 bonded atoms.

It is obvious that the percentage of differently coordinated atoms in the frozen layers has influence on the results of the central region. The samples initially containing a larger fraction of the sp^2 bonded atoms, contained a larger fraction of the sp^2 bonded atoms after cooling (at the same temperature of heating). Figure 13 shows the final percentage of sp^2 coordinated atoms as a function of heating "temperature" plotted for samples with different percentage of sp^3 and sp^2 bonded atoms before heating of the central layers. The data related to the smaller initial fraction of sp^2 atoms have a lower final fraction of the sp^2.

C. The band gap

During the calculations many samples of amorphous carbon with different structures were generated. The width of the band gap was "measured" for most of them by computing the density of states (DOS) as function of energy (energy levels are calculated in tight-binding molecular dynamics as

TABLE IV. The upper "temperature" of heating at which the sample reconstructed its diamond structure ($T*$) and percentage of sp^2 coordinated atoms in the samples cooled from 1.72 and 2.07 eV per atom.

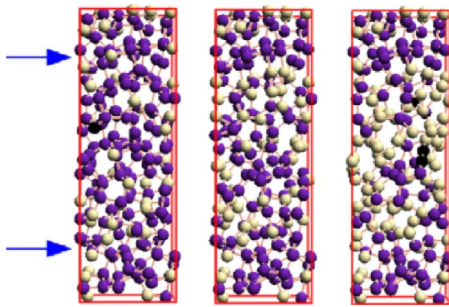| Width	$T*$	1.72 eV	2.07 eV
32 atoms	1.63 ± 0.04 eV	5 ± 5	20 ± 5
48 atoms	1.48 ± 0.04 eV	19 ± 5	32 ± 5
72 atoms	1.29 ± 0.04 eV	22 ± 5	41 ± 5

FIG. 10. (Color online) Samples of amorphous carbon located between two layers of $ta-C$ amorphous carbon: the initial sample (77.5% of sp^3) (left), and the samples after cooling from 2.07 eV (in the center), and from 2.33 eV (right). Grey (purple) balls represent fourfold coordinated atoms, white (yellow) balls represent threefold coordinated atoms, black balls (of which there are only four in the rightmost sample) represent twofold coordinated atoms. Boundaries between frozen layers and layers of atoms which are free to move are denoted by arrows. (Purple and yellow are shown online)

a result of diagonalization of the Hamiltonian matrix). For example, the graph of density of states for two samples of amorphous carbon, containing 86% of sp^3 bonded atoms and 53% of sp^3 bonded atoms is plotted in Fig. 14. The band gap of the sample with 86% of sp^3 bonded atoms was estimated visually from the graph to be 2.3 eV. The sample with 53% of sp^3 bonded atoms does not indicate the presence of any band gap, this sample is expected to be electrically conducting. The width of the band gap depends not only on the fraction of the differently coordinated atoms, but also on their individual configuration, i.e., on the local clustering of sp^2 bonded atoms. Figure 15 shows a plot of the width of the band gap as a function of the fraction of sp^3 coordinated atoms in various $ta-C$ samples.

There is a noticeable scattering of the points between 60% and 75% of sp^3 bonded atoms. We suspect that in this inter-
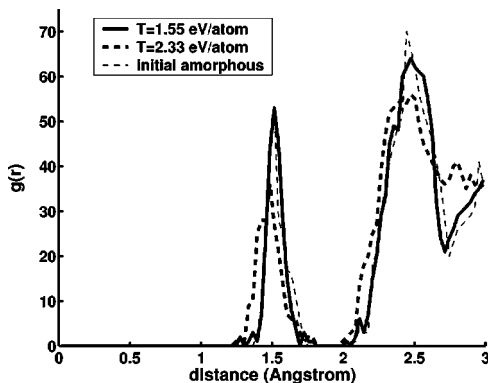

FIG. 11. Radial distribution functions $g(r)$ of the central layers of the sample containing 77.5% of sp^3 coordinated atoms initially (79% of sp^3 in the central layers), cooled from two different "temperatures:" after cooling from 1.55 eV the central layers contained 78% of sp^3 coordinated atoms, while after cooling from 2.33 eV the central layers contained 39% of sp^3 coordinated atoms. The thin dashed line shows the radial distribution function of the initial amorphous sample before heating for comparison.
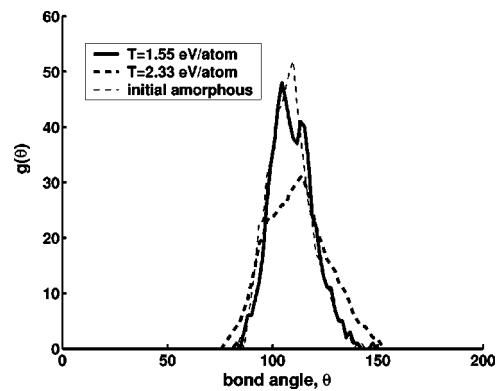

FIG. 12. Angular distribution function of the central layers of the sample containing 77.5% of sp^3 coordinated atoms initially (79% of sp^3 in the central layers), cooled from two different "temperatures." The thin dashed line shows the angular distribution function of the initial amorphous sample before heating for comparison.

val the fraction of sp^2 bonded atoms increases sufficiently to begin to create clusters. If the fraction of the sp^2 atoms is smaller than 25%, then only separated sp^2 bonded atoms are embedded in the sp^3 amorphous network. If the fraction of the sp^2 atoms is larger than 40%, the sp^2 clusters begin to connect one with another. The band gap disappears when the fraction of the sp^2 bonded atoms reaches 45%.

V. DISCUSSION AND COMPARISON WITH EXPERIMENT

The experimental results[1,5,36] described earlier show that the high local energy deposition of the ions into diamond or amorphous carbon along their paths causes a rearragement of
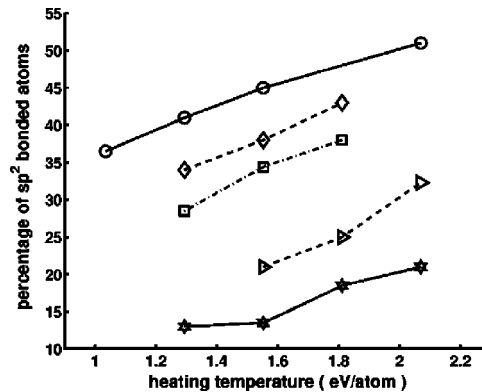

FIG. 13. The final percentage of sp^2 coordinated atoms as a function of heating "temperature" plotted for samples with different percentage of sp^3 and sp^2 bonded atoms before heating of the central layers. Circles in solid line are 38% of sp^2 in initial amorphous sample (36% in the central layers), diamonds in dashed line are 36% of sp^2 in initial amorphous sample (31% in the central layers), squares in dashed-doted line are 30% of sp^2 in initial amorphous sample (27.5% in the central layers), triangles in dashed line are 22.5% of sp^2 in initial amorphous sample (21% in the central layers), stars in solid line are 16% of sp^2 in initial amorphous sample (14% in the central layers).
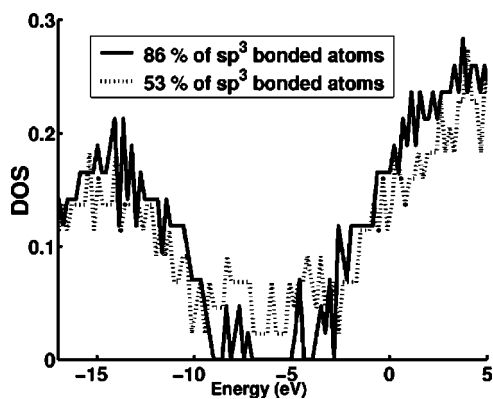
FIG. 14. The density of states of the samples of amorphous carbon, containing 86% of sp^3 bonded atoms and 53% of sp^2 bonded atoms. ($E=0$ is chosen arbitrary.)

the carbon atoms and can lead to a transformation of the insulating diamond or amorphous diamondlike sp^3 form of carbon into a conducting layer rich in sp^2 bonded carbon atoms. In the simulations we modeled the transformation of highly ordered diamond structures into amorphous structures with the presence of graphiticlike sp^2 bonds. In the samples which were initially amorphous, rearragement of the amorphous structure and an increase of the fraction of sp^2 bonded atoms has occurred.

The experiments[5,36] show that the resistivity, both in diamond and in amorphous carbon networks, decreases with ion dose. In diamond there exists a critical damage density D_c below which the diamond is restored to this pristine structure after annealing.[37] At $D=D_2$ a sharp drop in resistivity is observed and at higher doses graphitic conduction is measured in the irradiated volume. Kalish *et al.*[38] investigated the possibility that the sharp drop in resistivity could be explained in terms of a percolation transition between conducting islands produced by the impinging ion, but found that the R vs D dependence was not sharp enough to be consistent with such a simple percolation theory. By contrast, Hoffman *et al.*[39] in their experiment on 1 keV Ar irradiated diamond proved that the amorphization is a very sudden process and at D_2 the diamond collapses to an amorphous but still highly insulat-

ing form similar to amorphous diamond ($ta-C$). Only at doses exceeding those required for amorphization, does the amorphous sp^3 structure transform to an amorphous sp^2 structure which is electrically conducting. In our simulation at low "heating" temperatures the diamond also reconstructs this structure after cooling. At higher heating "temperatures" the structure remains amorphous after cooling and the fraction of sp^2 bonded atoms in the damaged region increases with the heating "temperatures." An increasing of the heated volume lead to increasing of sp^2 fraction along this ion track and to an increase of conductivity.

Experimental results[36] show that in contrast to diamond, for $ta-C$ where no crystalline template exists, there is nothing to inhibit the sp^3 to sp^2 bond conversion, hence there is no reason to expect a critical dose at which a sharp increase in the electrical conductivity should start. Moreover, the decrease of the electrical resistivity in $ta-C$ occurs at much lower implantation dose than in diamond.[36] The results of electron energy-loss spectroscopy allows to estimate the fraction of sp^2 bonds, f, in ion implanted $ta-C$. At low ion doses, f increases linearly with dose. At a dose of 10^{14} ions/cm^2, f becomes less sensitive and increases only slightly with dose. In our calculation $ta-C$ becomes a conductor at much lower heating "temperatures" than diamond, this means that in contrast to $ta-C$, diamond needs an additional energy to break its crystal lattice and result in amorphization upon cooling.

The conductivity in our amorphous carbon samples deduced from the shrinkage of the band gap increases with percentage of sp^2 bonded atoms in the damaged region. This trend is in accord with experimental observations. It should be noted that the conductivities of the $a-C$ layers are not simply related to the percentage of sp^2 bonds in the sample. Samples with similar sp^2 fractions sometimes exhibit somewhat different electrical properties. The specific configuration of the sp^2 bonded carbon atoms, whether they are clustered or not, plays an important role in the globally measured electrical conductivity. Hence, the comparison of electrical conductivities of different samples with even identical sp^2/sp^3 fractions can usually not be done directly. Given these issues of accuracy with the band gap computations, here, we are mainly concerned with the general trends which do follow those observed by others. An example of a specific comparison is that McCulloch *et al.*[36] found a band gap of 2.5 eV at 85% of sp^3 bonded atoms (see Fig. 15, where this is shown together with our result).

VI. SUMMARY

We have simulated a damaged region occuring in diamond and in diamondlike amorphous carbon by local heating of a slab in the sample. The slab is of thickness comparable to that created by the "thermal spike" due to the passage of an energetic ion, followed by quenching back to low temperature. The "temperature" of the heating varied from 1.2 to 2.59 eV/atom (14 000–30 000 K). These are temperatures expected to prevail for very short times within the thermal spike, as deduced from the kinetic energies imparted to the lattice of the stopping material during the slowing
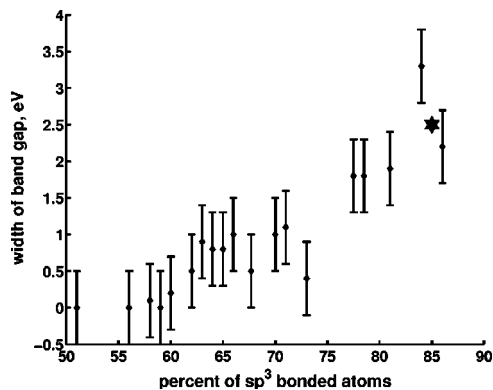

FIG. 15. The width of the band gap as a function of the percentage of sp^3 bonded atoms. The error bars represent an unaccuracy in visual determination of the band gap from DOS. The six-pointed star represent the result of McCulloch *et al.* for comparison.

down of an ion. For the case of diamond we found that at a heating "temperature" higher than a characteristic temperature T^* a small region in the center of the sample remains amorphous. The size and the structure of the amorphous region depends on the heating "temperature." Its size and the fraction of three- and two-coordinated atoms in the region increase with increase of the heating "temperature." When we increased the number of the free-to-move layers, the fraction of three- and two-coordinated atoms in the central layers increased. The curves of the dependence of the fraction of the sp^2 bonded atoms in the central layers on the temperature of heating have similar shape for different sizes of the hot layers.

The same procedure was applied to simulate a damaged region in amorphous carbon samples. The central layers of each sample were melted at very high temperatures (1.29–2.33 eV/atom) and then cooled by keeping the outer layers frozen. The percentage of three and twofold coordinated atoms in the obtained damaged region was found to increase with heating "temperature" and with the initial fraction of the threefold coordinated atoms in the sample. Most of the structures of amorphous carbon generated in different stages of our simulation were highly inhomogeneous and clustering of sp^2 bonded C atoms has been observed.

The band gap measured for all the amorphous carbon samples became narrower when the population of sp^2 bonded atoms increased. It vanished when the fraction of sp^2 bonded atoms reached a value of 45%. Beyond this fraction the damage affected volume becomes conductive.

The results obtained in this study support the experimental conclusions that in the damaged region formed after the passage of a heavy fast ion either through diamond or amorphous carbon, amorphization and sometimes conversion of sp^3 bonds to sp^2 bonds occurs. Another conclusion which follows from the simulations is that after passing of a faster (or heavier) ion (that corresponds to a higher temperature of the "thermal spike"), the damaged region is larger and more sp^3 bonds are transformed to sp^2. Although the present simulations do not exactly reproduce the conditions of the experimental "thermal spike," they include its dominant characteristics and qualitatively our results are in good agreement with experiments.

---

*Electronic address: anastasy@techunix.technion.ac.il; URL: http://phycomp.technion.ac.il/~anastasy/

[1] M. Waiblinger, Ch. Sommerhalter, B. Pietzak, J. Krauser, B. Mertesacker, M. Ch. Lux-Steiner, S. Klaumunzer, A. Weidinger, C. Ronning, and H. Hofsass, Appl. Phys. A: Mater. Sci. Process. **69**, 239 (1999).

[2] Reprinted from "Field emission enhancement by graphitic nanoscale channels through ta-C layers," N. Koenigsfeld, H. Hofsass, D. Schwen, A. Weidinger, C. Trautmann, and R. Kalish, Diamond Relat. Mater. **12**, 469 (2002), with permission from Elsevier.

[3] M. Dresselhaus and R. Kalish, *Ion Implantation in Diamond, Graphite and Related Materials* (Springer-Verlag, Berlin, 1992).

[4] J. F. Prins, Mater. Sci. Rep. **7**, 271 (1992).

[5] S. Prawer and R. Kalish, Phys. Rev. B **51**, 15 711 (1995).

[6] D. Saada, J. Adler, and R. Kalish, Phys. Rev. B **59**, 6650 (1999).

[7] J. F. Ziegler, SRIM-2003 http://www.srim.org

[8] J. Tersoff, Phys. Rev. Lett. **61**, 2879 (1988).

[9] N. A. Marks, D. R. McKenzie, B. A. Pailthorpe, M. Bernasconi, and M. Parinello, Phys. Rev. B **54**, 9703 (1996)

[10] G. Galli, R. Martin, R. Car, and M. Parinello, Phys. Rev. Lett. **62**, 555 (1989).

[11] F. Alvarez, C. C. Diaz, R. M. Valladarez, and A. A. Valladarez, Diamond Relat. Mater. **11**, 1015 (2002).

[12] C. Z. Wang, K. M. Ho, and C. T. Chan, Phys. Rev. Lett. **70**, 611 (1993).

[13] C. Z. Wang and K. M. Ho, Phys. Rev. Lett. **71**, 1184 (1993).

[14] T. Frauenheim, P. Blaudeck, U. Stephan, and G. Jungnickel, Phys. Rev. B **48**, 4823 (1993).

[15] F. Li and J. S. Lannin, Phys. Rev. Lett. **65**, 1905 (1990).

[16] S. Kugler, K. Shimakawa, T. Watanabe, K. Hayashi, I. László, and R. Bellissent, J. Non-Cryst. Solids **164–166**, 1143 (1993).

[17] P. C. Kelires, Phys. Rev. B **47**, 1829 (1993).

[18] D. R. McKenzie, D. Muller, and B. A. Pailthorpe, Phys. Rev. Lett. **67**, 773 (1991).

[19] P. J. Fallon, V. S. Veerasamy, C. A. Davis, J. Robertson, G. A. J. Amaratunga, W. I. Mine, and J. Koskinen, Phys. Rev. B **48**, 4777 (1993).

[20] Y. Lifshitz, Diamond Relat. Mater. **8**, 1659 (1999).

[21] W. Eckstein, *Computer Simulation of Ion-Solid Interactions* (Springer-Verlag, Berlin, 1991).

[22] M. Sha'anan, sstomy@sspower.technion.ac.il

[23] D. Rapaport, *The Art of MD Simulations* (Cambridge University Press, Cambridge, 1991).

[24] M. Posselt, Radiat. Eff. **130–131**, 87 (1994).

[25] Y. Zhang and G. Possnert, Nucl. Instrum. Methods Phys. Res. B **190**, 69 (2002).

[26] W. Wu and S. Fahy, Phys. Rev. B **49**, 3030 (1994).

[27] R. Smith, Proc. R. Soc. London, Ser. A **431**, 143 (1990).

[28] N. A. Marks, Phys. Rev. B **56**, 2441 (1997).

[29] J. F. Prins, T. E. Derry, and J. P. F. Sellschop, Phys. Rev. B **34**, 8870 (1986).

[30] C. Z. Wang, C. T. Chan, and K. M. Ho, Phys. Rev. B **39**, 8586 (1989).

[31] B. L. Zhang, C. H. Xu, C. Z. Wang, C. T. Chan, and K. M. Ho, Phys. Rev. B **46**, 7333 (1992).

[32] J. Adler, A. Hashibon, N. Schreiber, A. Sorkin, S. Sorkin, and G. Wagner, Comput. Phys. Commun. **147**, 665 (2002).

[33] http://phycomp.technion.ac.il/anastasy/newresult.html

[34] K. Binder, *Monte Carlo Methods in Statistical Physics* (Springer-Verlag, Berlin, 1986).

[35] I. Rosenblum, J. Adler, S. Brandon, and A. Hoffman, Phys. Rev. B **62**, 2920 (2000).

[36] D. G. McCulloch, E. G. Gerstner, D. R. McKenzie, S. Prawer, and R. Kalish, Phys. Rev. B **52**, 850 (1995).

[37] C. Uzan-Saguy, C. Cytermann, R. Brener, V. Richter, M. Sha'anan, and R. Kalish, Appl. Phys. Lett. **67**, 1194 (1999).

[38] R. Kalish, T. Bernstein, B. Shapiro, and A. Talmi, Radiat. Eff. **52**, 153 (1980).

[39] A. Hoffman, S. Prawer, and R. Kalish, Phys. Rev. B **45**, 12 736 (1992).